Adjustment of Twist Angles in Pseudo-Helical Lanthanide Complexes by the Size of Metal Ions

Shin Mizukami,*[a] Hirohiko Houjou,[a] Masatoshi Kanesato,*[a] and Kazuhisa Hiratani[b]

Abstract: Control of self-assembled nanostructures is a promising technique for nanotechnology. We have examined as to whether nanostructures could be controlled by the size of the central metal ion. Lanthanides are a natural choice for such a study as the size of their trivalent ions changes with atomic number gradually. For this investigation, a series of rare earth complexes ([LaL^1], [CeL^1], [SmL^1], [TbL^1], [YL^1], and [LuL^1]) with a tripodal heptadentate ligand L^1 were synthesized, and their X-ray crystallographic analysis was performed. Although the structures of the ligand (H_3L^1) and of the metal complex ([ML^1]) were quite different, all complexes were almost isostructural pseudohelices. The result of the crystallographic studies demonstrated that the twist angles of helices in the complexes depend on the ionic size of the central metal. A detailed analysis helped determine which portion of the helical strand contributed to the total helicity, and the major cause for the difference in helicity among the lanthanides is discussed. Moreover, this result is the first example showing that La^{III} and Lu^{III} complexes with the same tripodal heptadentate ligand are isostractural.

Keywords: helical structures · lanthanides · structure elucidation · twist angle

Introduction

In recent years, an increasing interest has been given to self-assembled supramolecular complexes with a strong hope to use them in nanotechnology.[1, 2] In particular, artificial construction of lanthanide supramolecular complexes is expected to generate new functional nanomaterials, because of their optical and magnetic properties.[3–5]

The fabrication of nanostructures containing lanthanide attracts our interests for another reason. The common coordination number for lanthanides is greater than that of the main transition metals.[6] The existence of complexes of lanthanides with larger coordination numbers is a natural consequence of their large size, and of the predominantly ionic character of their bonding. Therefore, lanthanide complexes have a strong potential for constructing various self-assembled structures. Bünzli and Piguet et al. reported the fabrication of triple-stranded helices by utilizing the large coordination numbers of lanthanide ions.[7, 8] It is very likely that the shape of such nanostructures can be controlled at will. Since the size of trivalent lanthanide ions decreases gradually with increasing atomic number, we expected that self-assembled structures could be controlled by changing the size of the metal ions. To verify the hypothesis, we synthesized a series of pseudo-helical, mononuclear rare earth complexes and investigated their structure.

Concerning pseudo-helical lanthanide complexes, Orvig and co-workers reported a ytterbium complex of tris(3-aza-4-methyl-6-oxohept-4-en-1-yl)amine.[9] Furthermore, some lanthanide derivatives of a range of Schiff base ligands of the type $N[CH_2CH_2N{=}CH(2\text{-}OH\text{-}3\text{-}R^1\text{-}5\text{-}R^2C_6H_2)]_3$ (H_3L) have also been reported.[10–12] In these complexes [ML] (M = Ce, Pr, Nd, Sm, Eu, Gd, Tb, Dy, Ho, Er, Tm, Yb, and Lu), each tripodal heptadentate Schiff-base ligand (L) effectively encapsulates the metal ion and enforces a seven-coordinate geometry. However, there has been no report about the structure of the La^{III} complexes. Since La^{III} has the largest ion radius and Lu^{III} has the smallest one among trivalent lanthanide ions, it was interesting to compare their structures. The structures of other lanthanide complexes are supposed to be intermediate between those of La^{III} and Lu^{III} complexes. Therefore, we tried to obtain single crystals of both La^{III} and Lu^{III} complexes with the same ligand.

We have been able to carry out the successful X-ray crystallographic analysis of seven-coordinate La^{III} and Lu^{III}

[a] Dr. S. Mizukami, Dr. M. Kanesato, Dr. H. Houjou
Nanoarchitectonics Research Center
National Institute of Advanced Industrial Science and Technology
Tsukuba Central 4, 1-1-1 Higashi, Tsukuba
Ibaraki 305-8562 (Japan)
Fax: (+81) 29-861-3029
E-mail: s-mizukami@aist.go.jp, m.kanesato@aist.go.jp

[b] Prof. K. Hiratani
Department of Applied Chemistry
Utsunomiya University
7-1-2 Youtou, Utsunomiya 321-8585 (Japan)

Supporting information for this article is available on the WWW under http://www.chemeurj.org or from the author.

  0947-6539/03/0907-1521 $ 20.00+.50/0

complexes by using a heptadentate pseudo-helical ligand. Furthermore, we obtained the crystal structures of several other metal (Ce^{III}, Sm^{III}, Tb^{III}, and Y^{III}) complexes with the same ligand, and we investigated their detailed crystal structure. In this paper, we also discuss the relationship between the metal ion radii and the twist angles of the helices. The results suggest that lanthanides could be used for the modulation of self-assembled structures.

Results and Discussion

At first, we synthesized a tripodal ligand (H_3L^1), which has a *tert*-butyl group at the 3-position of the salicylidene group as shown in Figure 1. We obtained a yellow single crystal by recrystallization from methanol and succeeded in analyzing

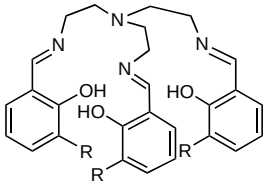

H_3L^1: R = *t*Bu
H_3L^2: R = H

Figure 1. Structures of tripodal heptadentate ligands.

the crystal structure. The unit cell contains two molecules of H_3L^1 that are crystallographically independent. Only the structure of one molecule is shown in Figure 2. The structure of the other molecule is almost the same as that of the first

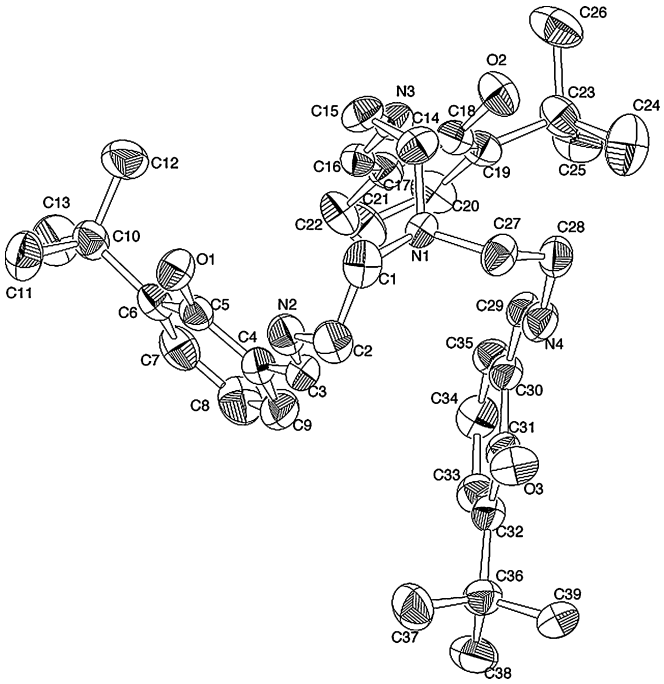

Figure 2. ORTEP diagram of H_3L^1. Thermal ellipsoids for the non-hydrogen atoms were drawn at the 50% probability level. Another molecule and hydrogen atoms were omitted for clarity.

one. The summary of the crystallographic data is presented in Table 1. It is notable that all hydroxyl and *tert*-butyl groups are oriented toward the outside probably because of steric hindrance.

Next, we synthesized various rare earth metal–L^1 complexes. Although yttrium is not among the lanthanides, its properties in coordination chemistry are quite similar to

Table 1. Crystallographic and experimental data for $[ML^1]$ (M = La, Ce, Sm, Tb, Y and Lu) and H_3L^1.

	$[LaL^1]$	$[CeL^1]$	$[SmL^1]$	$[TbL^1]$	$[YL^1]$	$[LuL^1]$	$(H_3L^1)_2$
formula	$C_{39}H_{51}LaN_4O_3$	$C_{39}H_{51}CeN_4O_3$	$C_{39}H_{51}N_4O_3Sm$	$C_{39}H_{51}N_4O_3Tb$	$C_{39}H_{51}N_4O_3Y$	$C_{39}H_{51}LuN_4O_3$	$C_{78}H_{108}N_8O_6$
M_r	762.75	763.96	774.21	782.77	712.75	798.81	1253.74
a [Å]	13.7486(3)	9.9335(5)	13.5039(5)	13.437(1)	13.388(1)	16.0668(3)	13.007(1)
b [Å]	13.7486(3)	14.1396(7)	14.6716(8)	14.641(1)	14.649(1)	13.0618(3)	23.396(2)
c [Å]	11.7137(3)	26.256(2)	19.1496(7)	19.146(1)	19.164(2)	18.4184(3)	12.8784(3)
α [°]	90	90	90	90	90	90	100.182(3)
β [°]	90	94.004(1)	97.639(2)	97.912(4)	98.105(4)	108.0976(7)	93.566(2)
γ [°]	120	90	90	90	90	90	81.835(1)
Z	2	4	4	4	4	4	2
V [Å^3]	1917.54(8)	3678.7(4)	3760.3(3)	3730.6(5)	3721.0(5)	3674.1(1)	3815.5(5)
ρ_{calcd} [g cm^{-3}]	1.321	1.379	1.368	1.394	1.272	1.444	1.091
crystal system	trigonal	monoclinic	monoclinic	monoclinic	monoclinic	monoclinic	triclinic
space group	$P\bar{3}$	$P2_1/c$	Cc	Cc	Cc	$P2_1/c$	$P\bar{1}$
crystal size [mm]	0.26 × 0.15 × 0.15	0.40 × 0.20 × 0.15	0.25 × 0.25 × 0.25	0.40 × 0.40 × 0.35	0.35 × 0.30 × 0.25	0.27 × 0.25 × 0.20	0.40 × 0.30 × 0.15
color, habit	light yellow, prism	red, block	light yellow, block	yellow, block	yellow, block	yellow, block	yellow, block
$2\theta_{max}$ [°]	54.9	55.0	55.0	54.9	55.0	55.0	55.0
measured reflections	18499	16933	18545	11595	17843	35004	35491
independent reflections	2940	7600	4294	3874	4244	8405	17143
	[R_{int} = 0.060]	[R_{int} = 0.071]	[R_{int} = 0.054]	[R_{int} = 0.043]	[R_{int} = 0.100]	[R_{int} = 0.049]	[R_{int} = 0.034]
μ [mm^{-1}]	1.148	1.278	1.605	1.932	1.610	2.728	0.069
reflections observed	2347	5729	3956	3763	3590	6377	8081
	[$I > 1.5\sigma(I)$]	[$I > 1.5\sigma(I)$]	[$I > 1.5\sigma(I)$]	[$I > 1.5\sigma(I)$]	[$I > 1.5\sigma(I)$]	[$I > 1.5\sigma(I)$]	[$I > 0$]
parameters	142	424	425	425	425	424	829
R[a]	0.0307	0.0476	0.0225	0.0227	0.0436	0.0244	0.0743
R_W[b]	0.0619	0.1090	0.0440	0.0688	0.0786	0.0411	0.1671

[a] $R = \Sigma||F_o| - |F_c||/\Sigma|F_o|$. [b] $R_w = [\Sigma w(F_o^2 - F_c^2)^2/\Sigma w(F_o^2)^2]^{1/2}$; $w = [\sigma^2(F_o^2)]^{-1}$.

0947-6539/03/0907-1522 $ 20.00+.50/0 *Chem. Eur. J.* **2003**, *9*, No. 7

theirs. Because the ion radius of Y^{III} is between those of Dy^{III} and Ho^{III},[6] it was expected that the structure of Y^{III} complexes are similar to those of these two lanthanides. The complexes were synthesized by methods A and B (Scheme 1).

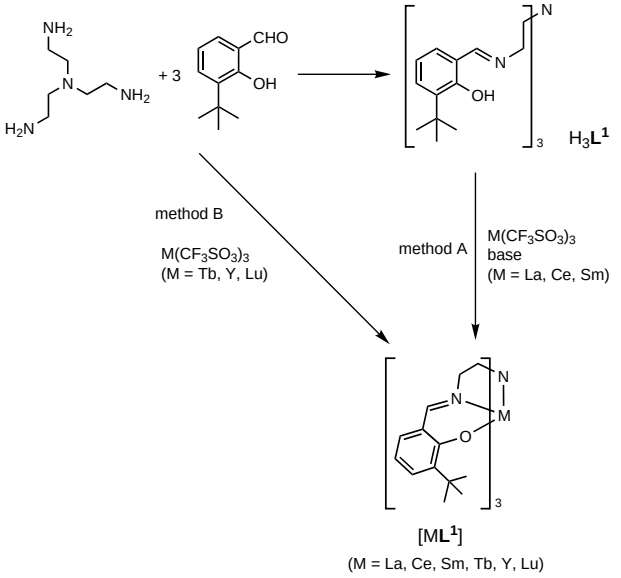

Scheme 1. Synthetic route of metal complexes.

In the case of $[LaL^1]$, $[CeL^1]$, and $[SmL^1]$, their complexes were synthesized from metal triflate and H_3L^1 in the presence of triethylamine (method A). The other metal complexes were prepared by metal template synthesis from tris(aminoethyl)amine, 3-*tert*-butylsalicylaldehyde and metal(III) triflate (method B). The use of a well-dried metal triflate salt was important for a good yield. The preparation yield was highest for $[TbL^1]$ (84%), and it got worse as the size of the central metal ion was further from that of the Tb^{III} ion, with the exception of cerium(III) complex. $[LaL^1]$ could not be obtained by method B, although $[SmL^1]$ could be. We were successful in obtaining single crystals of all complexes suitable for X-ray analysis through several procedures, and in determining their crystal structures. The crystallographic parameters are given in Table 1. The ORTEP drawings are given in Figure 3 ($[LaL^1]$, $[TbL^1]$, and $[LuL^1]$) and in the Supporting Information ($[CeL^1]$, $[SmL^1]$, and $[YL^1]$).

To our knowledge, there are no reports of La^{III} and Lu^{III} complexes with the same tripodal ligand that are isostructural. So far, an X-ray structure of a seven-coordinate La^{III} complex with a tripodal heptadentate ligand has never been observed. When we synthesized an La^{III} complex using L^2 (Figure 1) as the heptadentate ligand, we could not obtain single crystals of $[LaL^2]$. We thought that the coordination environment of $[LaL^2]$ was different from those of the other lanthanide(III) complexes $[ML^2]$, because the La^{III} ion is the largest among the lanthanide(III) ions and it might be coordinated by another donor atom in addition to the seven donor atoms of L^2. In the crystal structures of La^{III} complexes, there are numerous examples in which the solvent molecules or water molecules are also coordinated. In this work, we introduced *tert*-butyl groups at the *ortho*-position to the hydroxyl groups of the

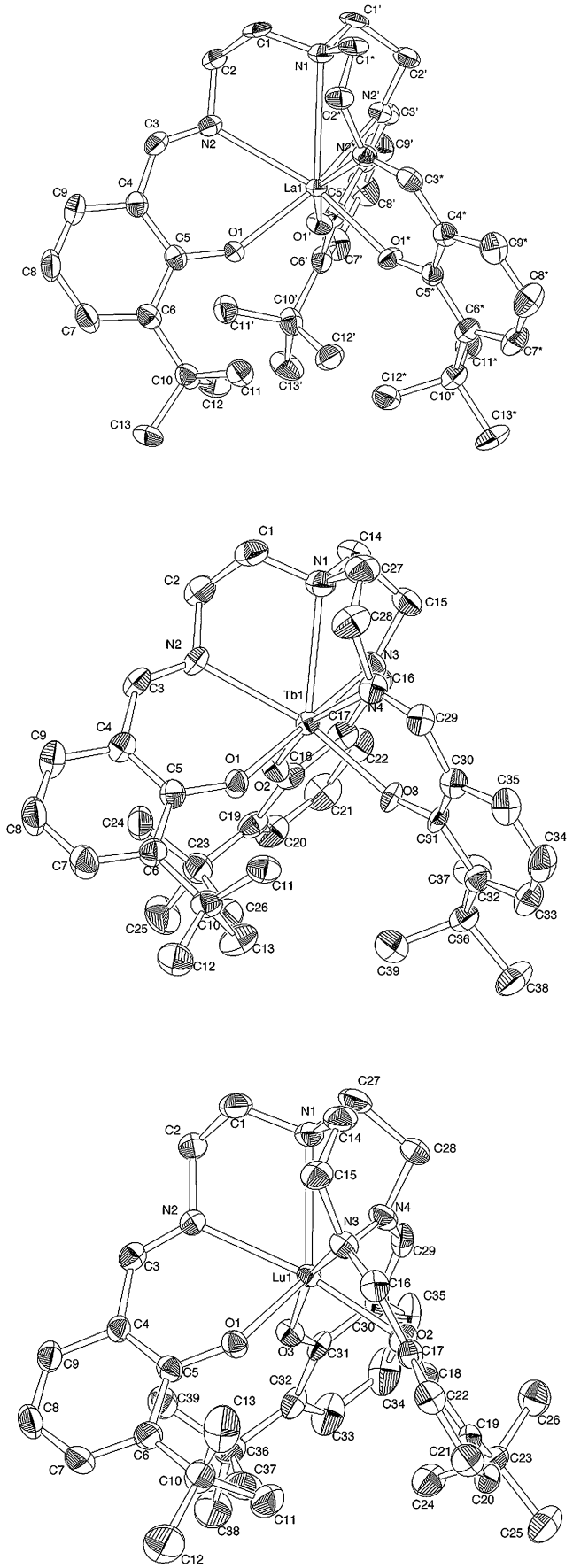

Figure 3. ORTEP diagram of $[LaL^1]$ (top), $[TbL^1]$ (middle), and $[LuL^1]$ (bottbom). Thermal ellipsoids for the non-hydrogen atoms were drawn at the 50% probability level. Hydrogen atoms were omitted for clarity.

  0947-6539/03/0907-1523 $ 20.00+.50/0

ligand to suppress the coordination of such molecules. We were then finally able to obtain a single crystal of the seven-coordinate complex [LaL^1].

As shown in the ORTEP drawings (Figure 3 and Supporting Information), all complexes [ML^1] (M = La, Ce, Sm, Tb, Y, and Lu) are seven-coordinate and pseudo-helical complexes. The structures of all metal complexes are quite different from that of H_3L^1, in which three hydroxyl groups are oriented toward the outside. Each central metal ion is coordinated by an apical nitrogen atom (N1) and three imino groups and three phenolic hydroxyl groups. [LaL^1] is C_3 symmetric, while other [ML^1] complexes are pseudo-C_3 symmetric. However, ^{1}H NMR spectra of [YL^1] and [LuL^1] showed that their structures are C_3 symmetric in solution. The distortion of their crystal structures is probably caused by crystal packing.

We compare now the detailed structures of the complexes on the basis of these crystallographic data. The selected bond lengths and bond angles of each [ML^1] are shown in Table 2. To facilitate the structural analysis, the simplified structure around metal ion of the complexes is shown in Figure 4a (view perpendicular to the C_3 axis (N1–M1) and b (view along the C_3 axis). The relationships between the ion radii of the central metal and the bond lengths M1–O1, M1–N1, and M1–N2 are shown in Figure 5. All metal–donor bond lengths decrease with the reduction of the lanthanide ion radius. The bond angles N1-M1-On (n = 1–3) are around 120° in all the complexes. Thus, these complexes are isostructural.

To study their solid structures more precisely, the average values of the bond angle Om-M1-On ($m \neq n$) are plotted against the ionic radii of the central metal in Figure 6. This value is almost independent of the ion radii of the central metal. We also compared the structures of the complexes along the C_3 axis (M1–N1) as shown in Figure 4b to determine their structural differences. All complexes appear to have similar triple pseudo-helices (Figure 3 and Supporting Information). However, we noticed that the twist angle values are different among the complexes. We at first selected the dihedral angle of C1-N1-M1-O1 as an index of twist angle. In

Table 2. Selected bond lengths [Å] and angles [°] in [LaL^1], [CeL^1], [SmL^1], [TbL^1], [YL^1], and [LuL^1].

La1–O1	2.330(2)	La1–N2	2.662(3)	La1–N1	2.984(4)		
O1-La1-O1*	93.08(8)	O1-La1-N2′	155.06(9)	O1-La1-N1	123.06(5)	N1-La1-N2	62.01(6)
O1-La1-N2	68.00(8)	N2-La1-N2*	99.76(7)	O1-La1-N2*	103.64(8)		
Ce1–O1	2.277(4)	Ce1–N2	2.605(5)	Ce1–O2	2.284(4)	Ce1–N3	2.638(5)
Ce1–O3	2.280(4)	Ce1–N4	2.649(4)	Ce1–N1	2.873(4)		
O1-Ce1-O2	91.8(1)	O3-Ce1-N1	119.6(1)	O1-Ce1-O3	101.2(1)	O3-Ce1-N2	99.3(1)
O1-Ce1-N1	120.7(1)	O3-Ce1-N3	157.5(1)	O1-Ce1-N2	68.8(1)	O3-Ce1-N4	68.8(1)
O1-Ce1-N3	93.8(1)	N1-Ce1-N2	64.0(1)	O1-Ce1-N4	169.4(1)	N1-Ce1-N3	64.2(1)
O2-Ce1-O3	94.3(1)	N1-Ce1-N4	64.2(1)	O2-Ce1-N1	122.9(1)	N2-Ce1-N3	101.7(1)
O2-Ce1-N2	158.1(1)	N2-Ce 1-N4	108.2(1)	O2-Ce1-N3	68.4(1)	N3-Ce1-N4	96.8(1)
O2-Ce1-N4	92.7(1)						
Sm1–O1	2.216(3)	Sm1–N2	2.565(4)	Sm1–O2	2.232(3)	Sm1–N3	2.549(4)
Sm1–O3	2.227(3)	Sm1–N4	2.542(4)	Sm1–N1	2.799(4)		
O1-Sm1-O2	95.3(1)	O3-Sm1-N1	121.1(1)	O1-Sm1-O3	97.0(1)	O3-Sm1-N2	166.6(1)
O1-Sm1-N1	119.8(1)	O3-Sm1-N3	91.5(1)	O1-Sm1-N2	70.3(1)	O3-Sm1-N4	70.6(1)
O1-Sm1-N3	164.1(1)	N1-Sm1-N2	64.9(1)	O1-Sm1-N4	90.1(1)	N1-Sm1-N3	65.7(1)
O2-Sm1-O3	93.8(1)	N1-Sm1-N4	65.6(1)	O2-Sm1-N1	123.2(1)	N2-Sm1-N3	101.9(1)
O2-Sm1-N2	91.7(1)	N2-Sm1-N4	104.3(1)	O2-Sm1-N3	70.6(1)	N3-Sm1-N4	105.4(1)
O2-Sm1-N4	164.0(1)						
Tb1–O1	2.206(4)	Tb1–N2	2.504(5)	Tb1–O2	2.192(4)	Tb1–N3	2.525(5)
Tb1–O3	2.216(4)	Tb1–N4	2.503(5)	Tb1–N1	2.761(6)		
O1-Tb1-O2	95.2(2)	O3-Tb1-N1	124.6(2)	O1-Tb1-O3	92.4(2)	O3-Tb1-N2	163.9(2)
O1-Tb1-N1	122.2(2)	O3-Tb1-N3	90.8(2)	O1-Tb1-N2	71.6(2)	O3-Tb1-N4	71.8(2)
O1-Tb1-N3	166.4(2)	N1-Tb1-N2	66.2(2)	O1-Tb1-N4	90.8(2)	N1-Tb1-N3	65.7(1)
O2-Tb1-O3	93.9(2)	N1-Tb1-N4	66.4(2)	O2-Tb1-N1	120.8(2)	N2-Tb1-N3	105.0(2)
O2-Tb1-N2	88.9(2)	N2-Tb1-N4	106.3(2)	O2-Tb1-N3	71.4(2)	N3-Tb1-N4	102.7(2)
O2-Tb1-N4	164.7(2)						
Y1–O1	2.164(5)	Y1–N2	2.484(5)	Y1–O2	2.177(4)	Y1–N3	2.468(6)
Y1–O3	2.161(4)	Y1–N4	2.493(5)	Y1–N1	2.771(6)		
O1-Y1-O2	92.6(2)	O3-Y1-N1	120.6(2)	O1-Y1-O3	94.0(2)	O3-Y1-N2	165.8(2)
O1-Y1-N1	124.4(2)	O3-Y1-N3	87.8(2)	O1-Y1-N2	72.6(2)	O3-Y1-N4	72.0(2)
O1-Y1-N3	164.9(2)	N1-Y1-N2	66.1(2)	O1-Y1-N4	89.8(2)	N1-Y1-N3	66.3(2)
O2-Y1-O3	96.0(2)	N1-Y1-N4	65.6(2)	O2-Y1-N1	121.8(2)	N2-Y1-N3	106.4(2)
O2-Y1-N2	89.6(2)	N2-Y1-N4	102.4(2)	O2-Y1-N3	72.3(2)	N3-Y1-N4	104.9(2)
O2-Y1-N4	167.9(2)						
Lu1–O1	2.124(2)	Lu1–N2	2.412(2)	Lu1–O2	2.153(2)	Lu1–N3	2.406(2)
Lu1–O3	2.158(2)	Lu1–N4	2.380(2)	Lu1–N1	2.658(2)		
O1-Lu1-O2	96.11(8)	O3-Lu1-N1	127.53(8)	O1-Lu1-O3	89.74(8)	O3-Lu1-N2	85.29(7)
O1-Lu1-N1	122.03(8)	O3-Lu1-N3	163.54(8)	O1-Lu1-N2	74.78(9)	O3-Lu1-N4	75.06(8)
O1-Lu1-N3	83.42(8)	N1-Lu1-N2	67.62(8)	O1-Lu1-N4	164.80(8)	N1-Lu1-N3	68.33(8)
O2-Lu1-O3	92.31(7)	N1-Lu1-N4	69.07(9)	O2-Lu1-N1	120.50(8)	N2-Lu1-N3	107.15(8)
O2-Lu1-N2	170.56(8)	N2-Lu1-N4	103.00(9)	O2-Lu1-N3	73.64(8)	N3-Lu1-N4	111.35(8)
O2-Lu1-N4	85.14(8)						

0947-6539/03/0907-1524 $ 20.00+.50/0 *Chem. Eur. J.* **2003**, *9*, No. 7

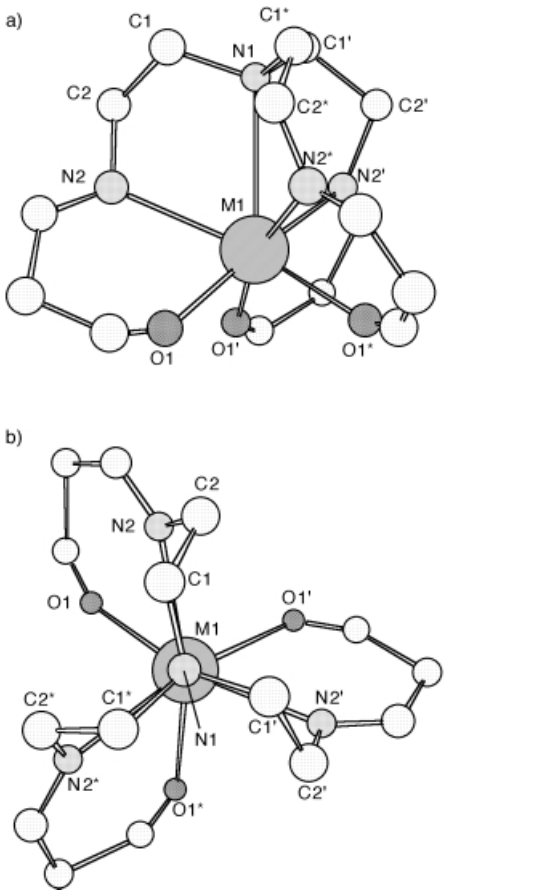

Figure 4. The simplified structure around the central metal ion of [ML^1]. a) The view perpendicular to the C_3 axis. b) The view along the C_3 axis. The atoms remote from the central metal ion were omitted for clarity.

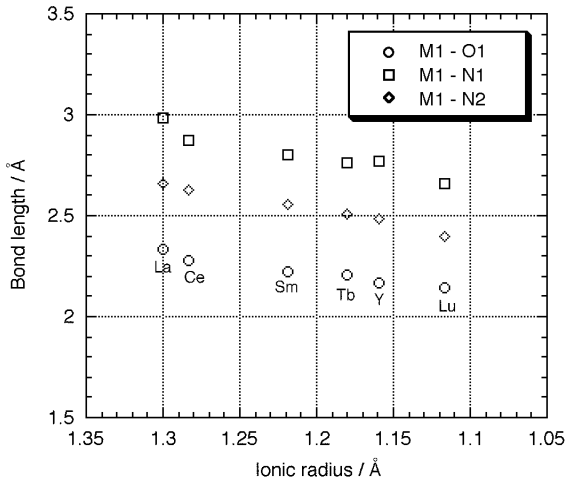

Figure 5. Relationship between metal ionic radii and bond lengths of [ML^1] (M = La, Ce, Sm, Tb, Y and Lu). The ionic radii data used were shown as crystal radii in case of eight-coordinate salt in reference [6].

Figure 6, the dihedral angles of C1-N1-M1-O1 (average values of three isotropic dihedral angles) are plotted against the ionic radii of the central metal. The twist angles increases with decreasing metal ionic size.

Next, to study in detail the difference of helicity, we analyzed the structures according to a method reported previously.[13] As shown in Figure 7, we partitioned the helical

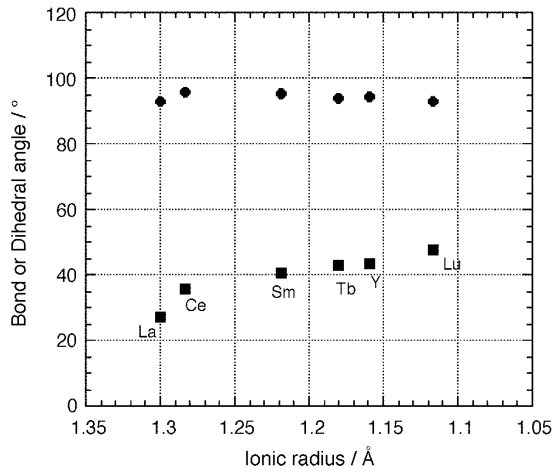

Figure 6. Relationship between the central metal ionic radii and bond or dihedral angles of [ML^1] (M = La, Ce, Sm, Tb, Y and Lu). Closed circles are the average value of the three O-M-O angles. Closed squares are the average value of three isotropic twist angles (dihedral angle of C1-N1-M1-O1) of each complex. The ionic radii data used were shown as crystal radii in case of eight-coordinate salt in reference [6].

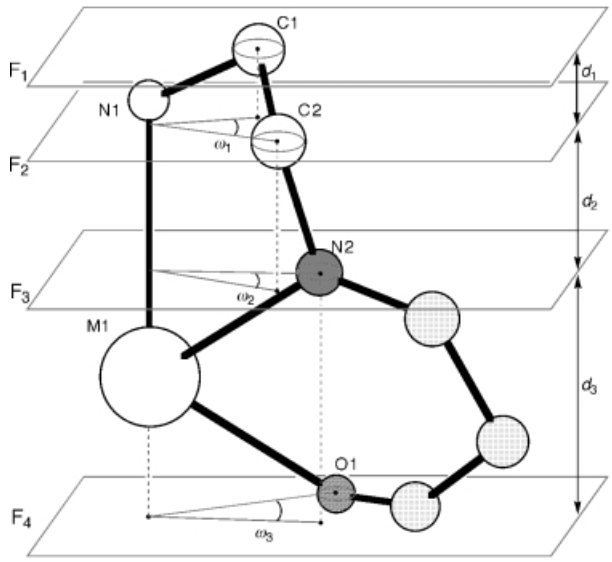

Figure 7. Definition of the partitioning planes F_i and of the parameters d_i and ω_i.

structure into three portions separated by four parallel planes F_1–F_4 to quantify the helical revolution about the C_3 axis and to calculate the helical pitch in each portion; F_1 is defined by the plane including three symmetrical atoms C1, C1′, C1* (or C1, C14, C27), F_2 by C2, C2′, C2* (or C2, C15, C28), F_3 by N2, N2′, N2* (or N2, N3, N4), and F_4 by O1, O1′, O1* (or O1, O2, O3). The distances (d_i) between these planes and the twist angle values (ω_i) in each portion are shown in Table 3; d_i is defined as the distance between F_i and F_{i+1}, and ω_1, ω_2, and ω_3 are defined as the averaged dihedral angles C1-N1-M1-C2, C2-N1-M1-N2, and N2-N1-M1-O1, respectively. Except for [LaL^1], each ω_i is the average value of three pseudo-symmetric angle values, for example, $\omega_1 = \{\measuredangle(\text{C1-N1-M1-C2}) + \measuredangle(\text{C14-N1-M1-C15}) + \measuredangle(\text{C27-N1-M1-C28})\}/3$.

Helical pitches P_i [Å] $= (d_i/\omega_i) \cdot 360$ calculated from the values of the two parameters, d_i [Å] and ω_i [°] are given in

Table 3. Distances (d_i) between partitioning planes (F_i) and the twist angles (ω_i) in each portion.

complex	ionic radius [Å] VII[a]	VIII[b]	d_1 [Å]	d_2 [Å]	d_3 [Å]	d_1+d_2 [Å]	$d_1+d_2+d_3$ [Å]	ω_1 [°]	ω_2 [°]	ω_3 [°]	$\omega_1+\omega_2$ [°]	$\omega_1+\omega_2+\omega_3$ [°]
[LaL^1]	1.24	1.300	0.878	1.326	2.518	2.204	4.722	−19.8	15.5	31.5	−4.3	27.3
[CeL^1]	1.21	1.283	0.906	1.323	2.324	2.229	4.553	−19.0	14.9	40.1	−4.1	35.9
[SmL^1]	1.16	1.219	0.906	1.326	2.219	2.232	4.451	−19.3	15.0	44.8	−4.3	40.4
[TbL^1]	1.12	1.180	0.916	1.324	2.197	2.240	4.437	−18.9	15.3	46.2	−3.6	42.5
[YL^1]	1.10	1.159	0.941	1.308	2.167	2.249	4.416	−18.7	15.6	47.6	−3.1	44.5
[LuL^1]	−−	1.117	0.929	1.329	2.064	2.258	4.322	−19.2	14.3	52.6	−4.9	47.7

[a] Ionic radius of the seven-coordinate metal.[6] [b] Ionic radius of the eight-coordinate metal.[6]

Table 4. Calculated helical pitches in each portion.[a]

complex	P_1 [Å]	P_2 [Å]	P_3 [Å]
[LaL^1]	−16.0	30.8	28.8
[CeL^1]	−17.2	32.0	20.9
[SmL^1]	−16.9	31.8	17.8
[TbL^1]	−17.4	31.2	17.1
[YL^1]	−18.1	30.2	16.4
[LuL^1]	−17.4	33.5	14.1

[a] A negative value means that the helix turns in the direction opposite to that of the total helicity.

Table 4. Figure 8 (top) shows that d_1 and d_2 hardly correlate with the ionic radii of the central metals, whereas d_3 decreases gradually with the lanthanide contraction. The twist angles ω_i are plotted similarly in Figure 8 (bottom). Although the first two angles ω_1 and ω_2 do not correlate either with the ionic radii of the metal, ω_3 increases with the lanthanide contraction. Since the sum of ω_1 and ω_2 is almost constant (around $-3°$ to $-5°$), the increase of dihedral angle C1-M1-N1-O1 ($=\omega_1+\omega_2+\omega_3$) with lanthanide contraction in Figure 6 results mainly from the contribution of ω_3. The same tendency is observed for P_i, that is, P_1 and P_2 are not correlated to the ionic size of the central metal, whereas P_3 decreases with the lanthanide contraction.

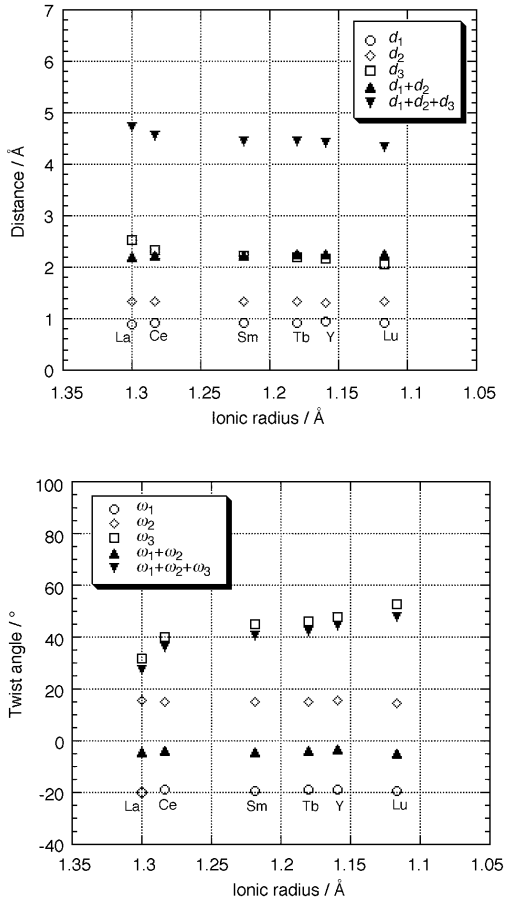

Figure 8. Relationship between the central metal ionic radii and distances d_i between partitioning planes (top), twist angles in each portion (bottom). The values of $\omega_1+\omega_2+\omega_3$ are equal to those of the dihedral angle C1-N1-M1-O1 in Figure 6. The ionic radii data used were shown as crystal radii in case of eight-coordinate salt in reference [6].

We consider now a possible cause for the increase of ω_3 when the lanthanide ionic radius decreases. It is notable from Figure 8 that the variation of ω_3 and d_3 are similar, albeit opposite, as a function of the lanthanide ionic radius. We have therefore plotted ω_3 and d_3 in Figure 9 and we observe that the

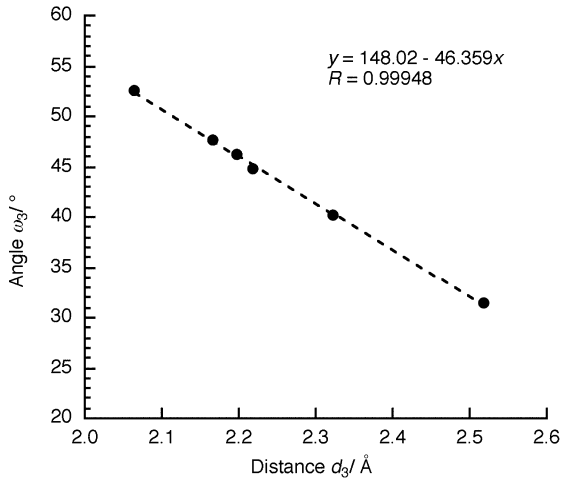

Figure 9. Correlation between d_3 and ω_3.

graph is linear. This result suggests that the decrease of d_3 causes the increase of ω_3, which almost equals the increase of the whole twist angle $\omega_1+\omega_2+\omega_3$. Since d_1+d_2 is almost constant (Table 3 or Figure 8 top), the effect of the lanthanide contraction is mainly reflected in d_3. As a result, the twist angle is maximum in [LuL^1] among all the lanthanide complexes studied in this work (Figure 10).

The above discussion clarifies the relationship between the twist angle of the complex [ML^1] and the ionic size of the lanthanides. This result implies that we can adjust the twist angle of helical complexes by using a proper ligand and metal ion. The data for the third helical pitch P_3 in Table 4 show that the value of P_3 for [LaL^1] is approximately twice as large as

0947-6539/03/0907-1526 $ 20.00+.50/0 *Chem. Eur. J.* **2003**, *9*, No. 7

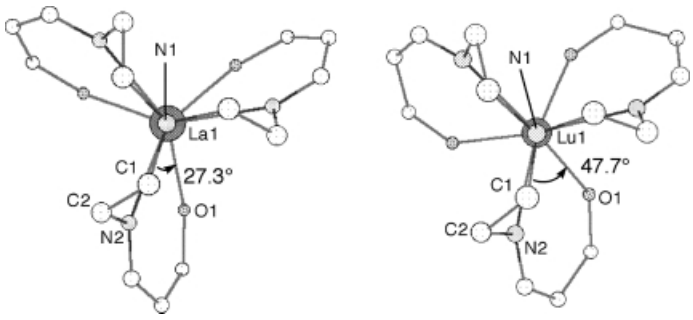

Figure 10. Schematic diagrams of [LaL^1] (left) and [LuL^1] (right). The dihedral angle (C1-M1-N1-O1) values were shown in this figure.

that of [LuL^1]. Therefore, we can control the length of helical nanostructures if the twist angles of helices can be adjusted.

Recently, several researchers reported the syntheses of helical complexes using self-assembly.[14, 15] Because lanthanide ions have a large coordination number, it will be advantageous to fabricate multiple helical nanostructures by using lanthanide complexes. Designing nanostructures with metal complexes, researchers were frequently unable to decide which metal ion should be useful. The results of this paper show the possibility that changing the metal ion would cause a fine control of self-assembled nanostructures.

Conclusion

We have reported the syntheses and the crystallographic studies of seven novel compounds; these are a ligand (H_3L^1) and six metal–ligand complexes ([LaL^1], [CeL^1], [SmL^1], [TbL^1], [YL^1], and [LuL^1]). This is the first example in which La^{III} and Lu^{III} complexes are isostructural when using the same tripodal heptadentate ligand. Therefore, we could make a systematic analysis of the crystal structures from La^{III} to Lu^{III}. Although the complexes are almost similar, the dihedral angle, which corresponds to the twist angle of the helix, increases as the metal ion radius decreases (Figure 10). Furthermore, we partitioned the angle into three portions to carry out a more detailed analysis. The third angle ω_3, which is the dihedral angle O1-M1-N1-N2, is the main contributor to the total twist angle. Finally, it was shown that the shape of nanostructures such as the angles or pitches of helices could be adjusted finely by choosing an adequate lanthanide ion. In the future, we expect to be able to build micro- or submicrostructures composed of nanomodules, for example, helices or sheets, which could be designed at will.

Experimental Section

General Remarks: Proton and carbon nuclear magnetic resonance (^{1}H and ^{13}C NMR) spectra were recorded on Bruker AVANCE 500 spectrometers. Electrospray ionization mass spectra (ESI-MS) were recorded with a Waters 2690 separations module, micromass ZMD, and Waters 996 photodiode array detector.

Tris[4-(2-hydroxy-3-*tert*-butylphenyl)-3-aza-3-butenyl]amine (H_3L^1): A solution of 3-*tert*-butylsalicylaldehyde (1.07 g, 6.0 mmol) in methanol (5 mL) was added to a hot solution of tris(aminoethyl)amine (tren) (292 mg, 2.0 mmol) in methanol (25 mL, 60 °C). The solution was stirred at 60 °C for 45 minutes under Ar atmosphere. After cooling, the precipitate was filtered and dried in vacuo to leave a yellow powder (1.12 g, 90 %). The single crystal for X-ray crystal structure analysis was obtained by the recrystallization from methanol. ^{1}H NMR (500 MHz $CDCl_3$): $\delta = 1.14$ (s, 27H; *t*Bu), 2.85 (t, $^3J = 5.0$ Hz, 6H; CH_2), 3.52 (t, $^3J = 5.0$ Hz, 6H; CH_2), 5.80 (dd, $^3J = 7.7$, $^4J = 1.5$ Hz, 3H; H^4), 6.53 (t, $^3J = 7.7$ Hz, 3H; H^5), 7.28 (dd, $^3J = 7.7$, $^4J = 1.5$ Hz, 3H; H^6), 7.77 (s, 3H; CH), 14.46 ppm (s, 3H; OH); ^{13}C NMR (500 MHz, $CDCl_3$): $\delta = 29.7$, 35.2, 56.7, 58.5, 118.2, 119.0, 129.3, 130.6, 137.5, 160.8, 167.1 ppm; elemental analysis calcd (%) for $C_{39}H_{51}LaN_4O_3$: C 74.72, H 8.68, N 8.94; found: C 74.99, H 8.72, N 8.95; ESI-MS: *m*/*z*: 549 [M^++H], 571 [M^++Na].

La^{III} complex ([LaL^1]): Triethylamine (202 mg, 2.0 mmol) was added to a hot solution of tris[4-(2-hydroxy-3-*tert*-butylphenyl)-3-aza-3-butenyl]amine (H_3L^1; 313 mg, 0.50 mmol) and $La(CF_3SO_3)_3$ (293 mg, 0.50 mmol) in acetonitrile (50 mL, 80 °C). The reaction mixture was stirred for 5 minutes. The solution was concentrated to less than 10 mL, then the precipitate was filtrated. Recrystallization from acetonitrile gave slightly yellow crystals (140 mg, 37 %). The single crystal was suitable for X-ray analysis. ^{1}H NMR (500 MHz $CDCl_3$): $\delta = 1.28$ (s, 27H; *t*Bu), 2.85 (br, 6H; CH_2), 3.24 (br, 3H; CH_2), 4.11 (br, 3H; CH_2), 6.49 (t, $^3J = 7.5$ Hz, 3H; H^5), 7.01 (dd, $^3J = 5.8$, $^4J = 1.7$ Hz, 3H; H^4), 7.29 (dd, $^3J = 5.8$, $^4J = 1.7$ Hz, 3H; H^6), 8.15 ppm (s, 3H; CH); elemental analysis calcd (%) for $C_{39}H_{51}LaN_4O_3$: C 61.41, H 6.74, N 7.35; found: C 61.45, H 6.71, N 7.32; ESI-MS: *m*/*z*: 763 [M^++H].

Ce^{III} complex ([CeL^1]): Triethylamine (101 mg, 1.0 mmol) was added to a hot solution of H_3L^1 (157 mg, 0.25 mmol) and $Ce(CF_3SO_3)_3$ (147 mg, 0.25 mmol) in methanol (25 mL, 60 °C). The reaction mixture was stirred for 30 minutes under Ar atmosphere, then the solution was cooled down. After filtration, the orange solid was recrystallized from acetonitrile under Ar atmosphere to obtain a red crystals (24 %). A single crystal suitable for X-ray structure analysis was obtained from the filtrate after three days. Elemental analysis calcd (%) for $C_{39}H_{51}CeN_4O_3$: C 61.31, H 6.73, N 7.33; found: C 61.35, H 6.67, N 7.32; ESI-MS: *m*/*z*: 763 [M^+].

Sm^{III} complex ([SmL^1]): Triethylamine (202 mg, 2.0 mmol) was added to a hot solution of H_3L^1 (313 mg, 0.50 mmol) and $Sm(CF_3SO_3)_3$ (299 mg, 0.50 mmol) in methanol (25 mL, 60 °C). The reaction mixture was stirred for 5 minutes under Ar atmosphere, and then the solution was cooled down. After filtration, the yellow solid was recrystallized from acetonitrile to obtain a light yellow crystals (47 %). A single crystal suitable for X-ray structure analysis was obtained from the filtrate after two weeks. Elemental analysis calcd (%) for $C_{39}H_{51}N_4O_3Sm$: C 60.50, H 6.64, N 7.24; found: C 60.30, H 6.79, N 7.07; ESI-MS: *m*/*z*: 776 [M^++H].

Tb^{III} complex ([TbL^1]): A solution of tris(aminoethyl)amine (292 mg, 2.0 mmol) in methanol (5 mL) was added to a hot solution of $Tb(CF_3SO_3)_3$ (606 mg, 1.0 mmol) in methanol (25 mL, 60 °C). The reaction solution was stirred at 60 °C for 2 minutes under Ar atmosphere. Then, a solution of 3-*tert*-butylsalicylaldehyde (534 mg, 3.0 mmol) in methanol (5 mL) was added and stirred. After 5 minutes, the solution was cooled down. Yellow crystals, which were suitable for X-ray analysis, was filtered and washed with methanol and diethyl ether, then dried in vacuo (659 mg, 84 %). Elemental analysis calcd (%) for $C_{39}H_{51}N_4O_3Tb$: C 59.84, H 6.57, N 7.16; found: C 59.77, H 6.48, N 7.06; ESI-MS: *m*/*z*: 783 [M^++H].

Y^{III} complex ([YL^1]): The synthetic procedure was similar to that of [TbL^1]. Yellow crystals, which were suitable for X-ray analysis, was filtered and washed with methanol and diethyl ether, then dried in vacuo (58 %). ^{1}H NMR (500 MHz $CDCl_3$): $\delta = 1.09$ (s, 27H; *t*Bu), 2.87 (m, 6H; CH_2), 3.23 (d, $^2J = 12.5$ Hz, 3H; CH_2), 4.13 (m, 3H; CH_2), 6.49 (t, $^3J = 7.5$ Hz, 3H; H^5), 7.04 (dd, $^3J = 7.5$, $^4J = 1.8$ Hz, 3H; H^4), 7.25 (dd, $^3J = 7.5$, $^4J = 1.8$ Hz, 3H; H^6), 8.17 ppm (s, 3H; CH); elemental analysis calcd (%) for $C_{39}H_{51}N_4O_3Y$: C 65.72, H 7.31, N 7.67; found: C 65.37, H 7.24, N 7.85; ESI-MS: *m*/*z*: 713 [M^++H].

Lu^{III} complex ([LuL^1]): The beginning of the synthetic procedure was similar to that of [TbL^1]. After filtration, the filtrate was condensed, and yellow crystals were filtered (26 %). ^{1}H NMR (500 MHz $CDCl_3$): $\delta = 1.02$ (s, 27H; *t*Bu), 2.91 (m, 6H; CH_2), 3.25 (d, $^2J = 12.5$ Hz, 3H; CH_2), 4.15 (m, 3H; CH_2), 6.48 (t, $^3J = 7.4$ Hz, 3H; H^5), 7.04 (dd, $^3J = 6.0$, $^4J = 1.8$ Hz, 3H; H^4), 7.25 (dd, $^3J = 6.9$, $^4J = 1.8$ Hz, 3H; H^6), 8.16 (d, $^4J = 1.2$ Hz, 3H; CH); elemental analysis calcd (%) for $C_{39}H_{51}LuN_4O_3$: C 58.64, H 6.44, N 7.01; found: C 58.32, H 6.38, N 6.92; ESI-MS: *m*/*z*: 799 [M^++H].

X-ray crystallographic study: The crystal data for all compounds were recorded on a Rigaku RAXIS-RAPID imaging plate diffractometer with

  0947-6539/03/0907-1527 $ 20.00+.50/0

graphite-monochromated $Mo_{K\alpha}$ radiation ($\lambda = 0.7107$ Å). All data were collected at $-80\,^{\circ}C$ in the ω-2θ mode. The crystal and experimental data are listed in Table 1. The structures were solved by direct methods and expanded by Fourier techniques. All non-hydrogen atoms were refined anisotropically. Absorption corrections were carried out for all data except those for H_3L^1. All of the structural analysis and adjustment were performed with the teXsan crystallographic software package (Molecular Structure Corporation).

CCDC-194616 to CCDC-194621 and CCDC-197760 contain the supplementary crystallographic data for this paper. These data can be obtained free of charge via www.ccdc.cam.ac.uk/conts/retrieving.html or from the Cambridge Crystallographic Data Centre, 12, Union Road, Cambridge CB2 1EZ, UK; fax: +44–1223–336–033; E-mail: deposit@ccdc.cam.ac.uk.

[1] G. F. Swiegers, T. J. Malefetse, *Chem. Rev.* **2000**, *100*, 3483–3537.
[2] B. J. Holliday, C. A. Mirkin, *Angew. Chem.* **2001**, *113*, 2076–2097; *Angew. Chem. Int. Ed.* **2001**, *40*, 2022–2043.
[3] V. Alexander, *Chem. Rev.* **1995**, *95*, 273–342.
[4] J.-C. G. Bünzli, C. Piguet, *Chem. Rev.* **2002**, *102*, 1897–1928.
[5] C. Benelli, D. Gatteschi, *Chem. Rev.* **2002**, *102*, 2369–2387.
[6] R. D. Shannon, *Acta Crystallogr. Sect. A* **1976**, *32*, 751–767.
[7] M. Elhabiri, R. Scopelliti, J. -C. G. Bünzli, C. Piguet, *J. Am. Chem. Soc.* **1999**, *121*, 10747–10762.
[8] B. Bocquet, G. Bernardinelli, N. Ouali, S. Floquet, F. Renaud, G. Hopfgartner, C. Piguet, *Chem. Commun.* **2002**, 930–931.
[9] D. J. Berg, S. J. Rettig, C. Orvig, *J. Am. Chem. Soc.* **1991**, *113*, 2528–2532.
[10] S. Liu, L. Gelmini, S. J. Rettig, R. C. Thompson, C. Orvig, *J. Am. Chem. Soc.* **1992**, *114*, 6081–6087.
[11] M. Kanesato, T. Yokoyama, O. Itabashi, T. M. Suzuki, M. Shiro, *Bull. Chem. Soc. Jpn.* **1996**, *69*, 1297–1302.
[12] M. Kanesato, T. Yokoyama, *Chem. Lett.* **1999**, 137–138.
[13] F. Renaud, C. Piguet, G. Bernardinelli, J. -C. G. Bünzli, G. Hopfgartner, *J. Am. Chem. Soc.* **1999**, *121*, 9326–9342.
[14] C. Piguet, G. Bernardinelli, G. Hopfgartner, *Chem. Rev.* **1997**, *97*, 2005–2062.
[15] M. Albrecht, *Chem. Rev.* **2001**, *101*, 3457–3498.

Received: October 10, 2002 [F4492]

  0947-6539/03/0907-1528 $ 20.00+.50/0